Exchange-correlation kernels for excited states in solids

Krzysztof Tatarczyk*, Arno Schindlmayr, and Matthias Scheffler
Fritz-Haber-Institut der Max-Planck-Gesellschaft, Faradayweg 4–6, 14195 Berlin-Dahlem, Germany
(February 1, 2008)

The performance of several common approximations for the exchange-correlation kernel within time-dependent density-functional theory is tested for elementary excitations in the homogeneous electron gas. Although the adiabatic local-density approximation gives a reasonably good account of the plasmon dispersion, systematic errors are pointed out and traced to the neglect of the wavevector dependence. Kernels optimized for atoms are found to perform poorly in extended systems due to an incorrect behavior in the long-wavelength limit, leading to quantitative deviations that significantly exceed the experimental error bars for the plasmon dispersion in the alkali metals.

PACS numbers: 71.45.Gm, 71.15.Mb, 71.10.Ca

I. INTRODUCTION

Exchange and correlation effects are crucial for understanding the properties of interacting many-electron systems but notoriously difficult to implement accurately in *ab initio* computational schemes. In the Kohn-Sham formulation of density-functional theory[1] they are incorporated into the exchange-correlation potential, which is a functional of the electron density but in practice is not known exactly except for simple model systems. Hence approximations such as the local-density or generalized gradient approximations are needed. In many cases these yield accurate total energies and related ground-state quantities.[2] However, the development of experimental devices that allow, in principle, to track a single electron and the emergence of new fields such as surface photochemistry place increasing emphasis on the study of *excited* states. Unfortunately its variational foundation prevents a straightforward application of the Kohn-Sham scheme to electronic excitations, for which numerically expensive Green function techniques or, in case of small systems, quantum-chemical methods were traditionally employed.

Time-dependent density-functional theory[3] promises an appealing alternative. Originally designed to explore time-dependent phenomena, it was recently realized that it can also be exploited to investigate optical excitations, which involve the creation of electron-hole pairs.[4] These are to be distinguished from photoemission states, which can be determined by calculating the self-energy correction to the quasiparticle band structure, for instance in the *GW* approximation.[5] The optical excitation energies correspond to the poles of the full linear density-response function, which can, in principle, be obtained exactly within time-dependent density-functional theory. This approach has since been applied to excited states not only in the context of quantum chemistry[4,6–8] but also, more recently, in solid-state physics.[9–13] The procedure starts from time-independent ground-state properties, such as the Kohn-Sham orbitals and eigenvalues, which are conveniently obtained by conventional means. However, besides static exchange and correlation embodied in the exchange-correlation potential, *dynamic* effects due to the time-dependent perturbation must also be accounted for. The latter are described by the so-called exchange-correlation kernel. Formally the kernel is a functional derivative of the exchange-correlation potential, evaluated at the unperturbed ground-state density, but as the exact potential is unknown and must in practice be approximated by a parameterization, independent expressions are often used for both quantities.

Chemical studies have repeatedly emphasized that an accurate description of the exchange-correlation potential is particularly important for excited-state calculations of atoms and molecules.[14–16] Although the local-density and generalized gradient approximations often yield good total energies, the corresponding potentials fail to capture the correct Coulomb-like asymptotic behavior and instead decay exponentially. As a result, many unoccupied states that really should be bound are pushed to higher energies and merge with the continuum. The accessible excitation spectrum is then poorly rendered. Much effort is therefore invested into better expressions for the exchange-correlation potential. In comparison, the kernel is considered to be less important, and the adiabatic local-density approximation is often chosen for convenience.

It is not clear whether these findings apply equally to solids. First, the problem of possible unbound states becomes irrelevant in bulk materials. Second, nonlocal dynamic exchange and correlation effects, which are neglected in the adiabatic local-density approximation, naturally become more prominent in extended systems with delocalized wavefunctions. For solids the errors introduced by approximations for the potential and the kernel could therefore be of similar magnitude. However, although several new parameterizations for the kernel were recently proposed in the literature,[4,16,17] these have not yet been systematically applied to solids, despite first encouraging attempts.[9] In fact, almost all calculations reported so far, which focus either on the dielectric response of semiconductors[9,10] or the plasmon dispersion in simple[11,12] and noble[13] metals, employ the local-density approximation both in the potential and the kernel. In

contrast to atoms, this approach seems to work reasonably well for solids, but improvements are still desirable.

In order to understand and quantify the error introduced by approximations to the kernel, more detailed studies for solids are necessary. Lein and co-workers[18] have recently compared the correlation energy of the homogeneous electron gas for different parameterizations, but the energy is an integrated quantity that principally reflects average weight distributions and is less sensitive to variations in the small-scale structure of the kernel. However, the latter have a significant influence on the excitation spectrum, which is given by the position of poles in the linear density-response function. In this paper we therefore concentrate on the dispersion relations for the plasmon frequency and lifetime, assessing the performance of several kernels currently circulated in the literature. By applying them to the homogeneous electron gas, where the exchange-correlation potential is a trivial constant, we are able to isolate the error due to the kernel and make a systematic comparison. Indeed, we find that the choice of parameterization plays an important role, and that inappropriate kernels optimized for atoms give rise to quantitative deviations that significantly exceed the experimental error bars for the plasmon dispersion in the alkali metals. We believe that the findings presented in this paper can not only be extended to plasmons in real materials but generally apply to excited states in solids that, like plasmons, are based on charge rearrangements. A prominent example are charge-transfer excitations in surface-adsorbate systems that occur during photoinduced reactions.[19]

This paper is organized as follows. In Sec. II we give an outline of our computational method. The kernels considered here are listed in Sec. III, and in Sec. IV we present the numerical results together with a discussion. Finally, in Sec. V we summarize our conclusions. Rydberg atomic units are used throughout.

II. COMPUTATIONAL METHOD

Within linear response theory the true many-body density-density response function is defined as

$$\chi(\mathbf{r},\mathbf{r}';t-t') = \frac{\delta n(\mathbf{r},t)}{\delta V^{\rm ext}(\mathbf{r}',t')} \;, \tag{1}$$

where $\delta n(\mathbf{r},t)$ indicates the density change induced by an external perturbation $\delta V^{\rm ext}(\mathbf{r}',t')$, and the functional derivative is evaluated at the static external potential corresponding to the unperturbed ground-state density. Likewise, the Kohn-Sham susceptibility

$$\chi^0(\mathbf{r},\mathbf{r}';t-t') = \frac{\delta n(\mathbf{r},t)}{\delta V^{\rm eff}(\mathbf{r}',t')} \;, \tag{2}$$

describes the response of the associated noninteracting system with the same electron density due to a change $\delta V^{\rm eff}(\mathbf{r}',t') = \delta V^{\rm ext}(\mathbf{r}',t') + \delta V^{H}(\mathbf{r}',t') + \delta V^{\rm xc}(\mathbf{r}',t')$ in the effective potential, which includes the Hartree and exchange-correlation contributions. It can be calculated explicitly in frequency space according to

$$\chi^0(\mathbf{r},\mathbf{r}';\omega) = 2\sum_{\nu,\nu'}(f_{\nu'}-f_\nu)\frac{\varphi_\nu(\mathbf{r})\varphi^*_{\nu'}(\mathbf{r})\varphi^*_\nu(\mathbf{r}')\varphi_{\nu'}(\mathbf{r}')}{\omega-(\epsilon_\nu-\epsilon_{\nu'})+i\eta} \tag{3}$$

from the static Kohn-Sham orbitals φ_ν and eigenvalues ϵ_ν. The symbol f_ν indicates the Fermi occupation numbers and η is a positive infinitesimal. The true density-density response function is obtained by relating it to the Kohn-Sham susceptibility through the chain rule for functional derivatives, which may be written in the form

$$\int d^3r''\, M(\mathbf{r},\mathbf{r}'';\omega)\chi(\mathbf{r}'',\mathbf{r}';\omega) = \chi^0(\mathbf{r},\mathbf{r}';\omega)\;. \tag{4}$$

The operator

$$M(\mathbf{r},\mathbf{r}';\omega) = \delta(\mathbf{r}-\mathbf{r}') - \int d^3r''\,\chi^0(\mathbf{r},\mathbf{r}'';\omega) \times\left(\frac{1}{|\mathbf{r}''-\mathbf{r}'|}+f^{\rm xc}(\mathbf{r}'',\mathbf{r}';\omega)\right) \tag{5}$$

is related to the dielectric function and the exchange-correlation kernel is defined as

$$f^{\rm xc}(\mathbf{r},\mathbf{r}';t-t') = \frac{\delta V^{\rm xc}(\mathbf{r},t)}{\delta n(\mathbf{r}',t')} \;, \tag{6}$$

where the functional derivative is evaluated at the unperturbed ground-state density.

The many-body density-density response function has poles at the exact excitation energies of the interacting electron system. On the other hand, χ^0 has poles at the excitation energies of the corresponding Kohn-Sham system, which are in general different. Hence the singularities of χ in Eq. (4) must be cancelled by zeroes of the operator M. Independent of the system characteristics and the nature of the excited states, this provides a convenient starting point for calculating the excitation spectrum. For atoms it is possible to expand all quantities in a Laurent series around a particular Kohn-Sham energy difference $\epsilon_\nu-\epsilon_{\nu'}$, which leads to an explicit expression for low-order corrections to the transition energy.[4] This procedure is not appropriate for solids, however, because in infinite systems the Kohn-Sham transition energies form a continuum.[20] Although the resulting structure of χ^0 can still be described in terms of effective poles, these are located off the real axis and no longer correspond to individual energy differences in the denominator of Eq. (3). For the homogeneous electron gas we therefore determine the plasmon dispersion $\Omega(q)$ by a direct search for the zeroes of

$$M(q,\omega) = 1-\chi^0(q,\omega)\,[v(q)+f^{\rm xc}(q,\omega)] \tag{7}$$

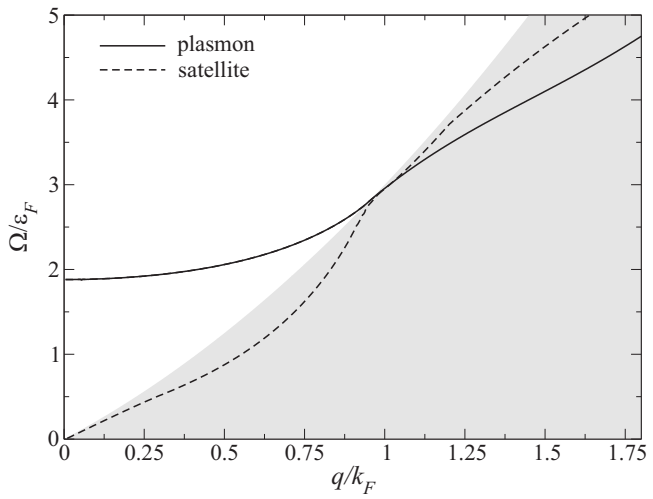

FIG. 1. At the border of the electron-hole pair continuum, indicated by the shaded region, a crossing between the plasmon dispersion and a satellite excitation occurs.

in reciprocal space, which is also the most accurate procedure. The Fourier transform of the Coulomb potential is $v(q) = 4\pi/q^2$, and the Kohn-Sham susceptibility χ^0 is given analytically by the dynamic Lindhard function.[21]

In our implementation we generally calculate the zeroes of M in the complex frequency plane, which allows us to obtain both the plasmon dispersion and the corresponding lifetimes. This approach requires the simultaneous solution of a set of two nonlinear equations for the real and the imaginary part, for which we employ an iterative procedure. At $q = 0$ the classical plasma frequency $\omega_p = (4\pi n)^{1/2}$ forms a convenient starting point, while for finite q the previously calculated solution for a smaller wavevector is utilized. We have confirmed that the iteration is stable and convergent. Special attention must be paid at $\Omega(q) = \frac{1}{2}q^2 + qk_F$, however, where the structure of the excitation spectrum becomes very complicated and a bifurcation occurs. This bifurcation, illustrated in Fig. 1 for the random-phase approximation and $r_s = 4$, where r_s denotes the Wigner-Seitz radius, is due to the crossing of the plasmon dispersion with a satellite excitation. In order to discriminate between the principal resonance and its satellite, we examine the spectral function

$$S(q,\omega) = -\frac{1}{nv(q)}\,\mathrm{Im}\,\frac{1}{M(q,\omega)} \tag{8}$$

on the real frequency axis, where the plasmon peak can easily be identified as the dominant feature.

The imaginary part of $\Omega(q)$ reflects the finite lifetime of plasmons in the homogeneous electron gas. The most important decay mechanism is scattering into electron-hole pairs, which dominates whenever energy and momentum conservation allow the promotion of an electron into a previously unoccupied state above the Fermi level.[20] This region, bounded by the two lines $\frac{1}{2}q^2 \pm qk_F$, where k_F denotes the Fermi wavevector, is shown shaded in Fig. 1. Real solutions for the plasmon energy, suggesting an infinite lifetime, only exist for frequency-independent kernels outside the electron-hole pair continuum. This behavior, well known from the random-phase approximation, constitutes a physically implausible artefact that stems from the neglect of more intricate decay channels.

III. EXCHANGE-CORRELATION KERNELS

In this paper we have considered the following approximations for the exchange-correlation kernel.

(a) In the random-phase approximation (RPA) all dynamic exchange-correlation effects are ignored by setting

$$f^{\mathrm{xc}}_{\mathrm{RPA}} = 0\,. \tag{9}$$

(b) The adiabatic local-density approximation[22] (ALDA) equals the long-wavelength limit

$$f^{\mathrm{xc}}_{\mathrm{ALDA}} = \lim_{q\to 0} f^{\mathrm{xc}}_{\mathrm{hom}}(q,\omega=0) \tag{10}$$

of the static exchange-correlation kernel of the homogeneous electron gas. It is readily expressed in terms of the exchange-correlation energy per particle $\epsilon^{\mathrm{xc}}_{\mathrm{hom}}$ as

$$f^{\mathrm{xc}}_{\mathrm{ALDA}} = \frac{d^2}{dn^2}\left[n\epsilon^{\mathrm{xc}}_{\mathrm{hom}}(n)\right]\,. \tag{11}$$

Owing to its computational simplicity, the ALDA has become the standard approximation in time-dependent density-functional theory. It has already been employed in calculations of the plasmon dispersion for solids.[11–13]

(c) In their original application of time-dependent density-functional theory to excited states, Petersilka, Gossmann, and Gross[4] (PGG) derived an approximate exchange-only kernel in the spirit of the optimized effective potential method.[23] This approach has the advantage that the corresponding exchange potential has the proper Coulomb decay. The kernel is constructed from the Kohn-Sham orbitals and hence only depends implicitly on the density. Designed for small atoms, the PGG formula is identical to the exact exchange kernel for two-electron systems, but deviations are expected for extended systems. In particular, the frequency dependence of the exact exchange kernel, which, in principle, can also be calculated,[24] is ignored. In momentum space the PGG kernel is given by[18]

$$f^{\mathrm{xc}}_{\mathrm{PGG}}(q) = -\frac{3\pi}{10k_F^2}\left\{11 + 2Q^2 + \left(\frac{2}{Q} - 10Q\right)\ln\frac{1+Q}{|1-Q|} + \left(2Q^4 - 10Q^2\right)\ln\left|1 - \frac{1}{Q^2}\right|\right\} \tag{12}$$

with $Q = q/2k_F$.

(d) Burke, Petersilka, and Gross[16] (BPG) recently proposed a hybrid formula that was shown to improve the excitation spectra of small atoms. It combines expressions

for symmetric and antisymmetric spin orientations from different approximations in a spin density-functional formalism. For the unpolarized homogeneous electron gas this kernel reduces to

$$f^{\rm xc}_{\rm BPG}(q) = \frac{1}{2}\left[f^{\rm xc}_{{\rm PGG},\uparrow\uparrow}(q) + f^{\rm xc}_{{\rm ALDA},\uparrow\downarrow}\right] . \qquad (13)$$

(e) An essentially exact parameterization of the static exchange-correlation kernel for the homogeneous electron gas was given by Corradini, Del Sole, Onida, and Palummo[17] (CDOP), who used the Monte Carlo results of Moroni, Ceperley, and Senatore[25] for the static local-field factor $G(q) = -f^{\rm xc}(q)/v(q)$. Unlike the original data, the fit

$$f^{\rm xc}_{\rm CDOP}(q) = -\frac{4\pi}{q^2}\left(CQ^2 + \frac{BQ^2}{g+Q^2} + \alpha Q^4 e^{-\beta Q^2}\right) \qquad (14)$$

with $Q = q/k_F$ is not restricted to metallic densities, because it incorporates the known asymptotic limits for high and low densities. The parameters α, β, B, C, and g depend on r_s and are listed in Ref. 17. By construction, the CDOP kernel becomes identical to the ALDA in the long-wavelength limit.

(f) Finally we consider a parameterization of the *dynamic* local-field factor of the homogeneous electron gas proposed by Richardson and Ashcroft[26] (RA), including the corrections given in Ref. 18, which stems from the summation of self-energy, exchange, and fluctuation terms in the diagrammatic expansion of the polarization function. It satisfies many important sum rules and includes exact asymptotic expressions for small and large wavevectors. At intermediate wavevectors and frequencies it provides a realistic description of the position and magnitude of extrema, which are related to the pair distribution function evaluated at zero separation. Because of this careful derivation we believe the RA expression to be very close to the exact dynamic exchange-correlation kernel of the homogeneous electron gas and give an accurate account of the plasmon dispersion. In the absence of experimental data we therefore use the RA results as a reference in order to assess the performance of simpler approximations. The parameterization

$$f^{\rm xc}_{\rm RA}(q,\omega) = -\frac{4\pi}{q^2}\left[G_s(Q,U) + G_n(Q,U)\right] \qquad (15)$$

with $Q = q/2k_F$ and $U = \omega/4k_F^2$ was originally given on the imaginary frequency axis, so we use a continuation to the full complex plane. The local-field factor G_s describes screened exchange, fluctuation, and self-energy effects in the irreducible polarizability, while G_n accounts for the change in occupation numbers due to correlation. The parameterized forms of both are listed in Ref. 26.

Whenever the exchange-correlation energy is needed as an input, we use the parameterization by Perdew and Wang[27] of the Monte Carlo data by Ceperley and Alder.[28] The pair-correlation function that enters the RA kernel is taken from the same authors.[29]

IV. RESULTS AND DISCUSSION

Before presenting our numerical results we first discuss what can be deduced from an analytic expansion of the plasmon dispersion $\Omega(q)$. By solving $M(q,\Omega(q)) = 0$ up to second order in q we obtain the series[2]

$$\Omega(q) = \omega_p\left[1 + \left(\frac{9}{10k_{\rm TF}^2} + \frac{f^{\rm xc}(0,\omega_p)}{8\pi}\right)q^2 + {\rm O}(q^4)\right] , \qquad (16)$$

where $k_{\rm TF}$ indicates the Thomas-Fermi wavevector. As long as $f^{\rm xc}$ does not diverge, all curves should approach the classical plasma frequency in the long-wavelength limit. The kernel only introduces corrections beyond the RPA in second order, where the element $f^{\rm xc}(0,\omega_p)$ appears. The ALDA evidently contains the right long-wavelength limit of the kernel, but its neglect of the frequency dependence still introduces an error in the parabolic term. By construction, the CDOP formula becomes identical to the ALDA in the long-wavelength limit and thus produces the same second-order term. Being static approximations, the PGG and BPG functionals are also evaluated at $\omega = 0$ rather than the plasma frequency. However, they do not approach the correct long-wavelength limit of the homogeneous electron gas and therefore generate a different parabolic coefficient. The RA kernel, which incorporates the full frequency dependence, is the only parameterization that is formally exact beyond the trivial zeroth order.

The numerically calculated plasmon dispersions for $r_s = 4$ are shown in Fig. 2. As predicted, all curves start at the classical plasma frequency. For small wavevectors only a small spread of the results is observed, because

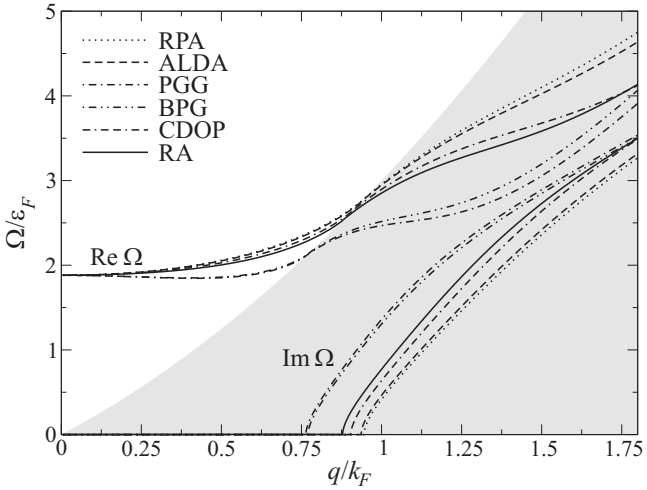

FIG. 2. Plasmon dispersion for the homogeneous electron gas at $r_s = 4$, calculated with different approximations for the exchange-correlation kernel. The electron-hole pair continuum and the resulting nonzero imaginary part of the plasmon frequency in this regime are also marked.

the factor $9/10k_{\mathrm{TF}}^2$ in Eq. (16) in general outweighs the contribution of the kernel. However, a slight downward shift compared to the RPA is clearly visible for all nontrivial approximations, because dynamic exchange and correlation effects combine to lower the energy of the electron system. The ALDA and the CDOP formula produce curves that are initially very close to the RA result we use for reference, indicating that the neglected frequency dependence is of little consequence as long as the correct long-wavelength limit is reproduced. This point is emphasized by the relatively large deviation for the static PGG kernel, which stems precisely from its incorrect behavior at $q \to 0$. The BPG curve, as expected, lies between the ALDA and PGG results.

To demonstrate that these observations are representative, in Fig. 3 we show the behavior of the plasmon energy over a large density range. The curves are calculated for $q = 0.5q_c$, where q_c indicates the critical wavevector corresponding to the onset of damping due to electron-hole pair excitations in the RPA. Note that the results are scaled in units of the Fermi energy ϵ_F, which is itself a function of r_s. The RPA and ALDA curves are practically indistinguishable on the scale of the figure. In the high-density limit all parameterizations tend to the RPA result, which is the correct trend. The deviation between the RA dispersion and the other curves increases approximately linearly with r_s.

At larger wavevectors, where the parabolic expansion (16) is no longer valid, the differences between the considered approximations become more pronounced. The dispersion resulting from the static ALDA kernel remains close to the RPA at too high energies, while the CDOP result begins to deviate slightly from the RA curve after the onset of damping in the electron-hole pair continuum. This discrepancy must be attributed to the static nature

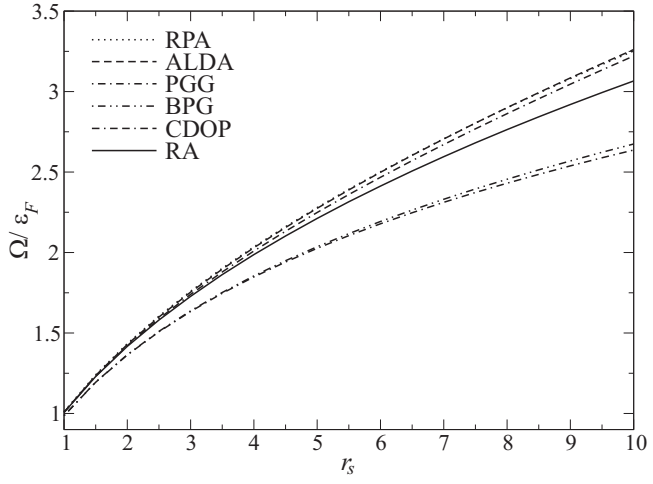

FIG. 3. Behavior of the plasmon energy as a function of the density evaluated at $q = 0.5q_c$, where q_c indicates the critical wavevector corresponding to the onset of damping due to electron-hole pair excitations in the RPA.

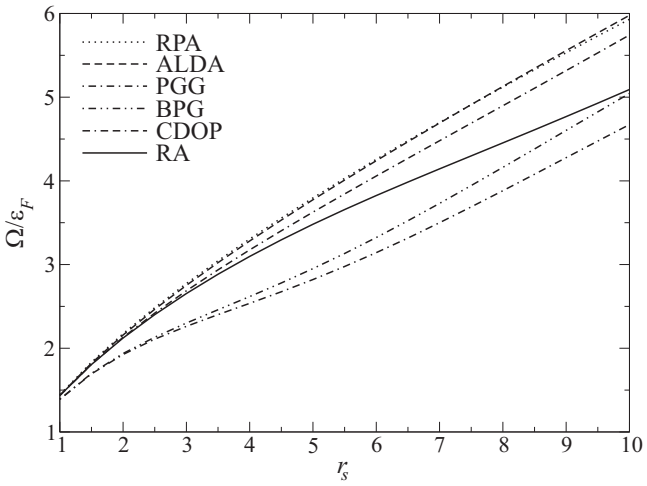

FIG. 4. Behavior of the plasmon energy in the region of electron-hole pair excitations at $q = 1.2q_c$.

of the CDOP kernel. Furthermore, it can be seen that the strong downward shift of the exchange-only PGG formula leads to an even larger error in absolute terms than the underestimation of dynamic exchange and correlation effects in both the ALDA and RPA. The hybrid BPG formula, which combines the PGG and ALDA parameterizations, profits from a partial cancellation of errors but improves only marginally upon PGG. In Fig. 4 we again show the plasmon energy as a function of the density for $q = 1.2q_c$.

Due to decay into electron-hole pairs in the damped regime, the plasmon energy acquires a nonzero imaginary part, also displayed in Fig. 2, whose inverse is proportional to the lifetime. As a general rule we find that all kernels yield the same quality of approximation for the imaginary part as they do for the real part of the plasmon energy. At small wavevectors, as discussed above, static kernels predict a vanishing imaginary part, which corresponds to an unphysical infinite lifetime. This artefact results from modelling f^{xc} as a purely real quantity by evaluating it at $\omega = 0$. In fact, the exact kernel has a finite imaginary part at nonzero frequencies, which for small wavevectors is related to the multi-pair component of the susceptibility according to[30]

$$\mathrm{Im}\, f^{\mathrm{xc}}(q,\omega) \approx -\frac{\omega^4}{\omega_p^4}[v(q)]^2\, \mathrm{Im}\, \chi^{\mathrm{mp}}(q,\omega)\,. \qquad (17)$$

Such multi-pair decay channels are ignored in the RPA and related schemes, which is ultimately the reason for their qualitatively wrong behavior. Mermin's modification of the Lindhard dielectric function avoids the problem of infinite lifetimes,[31] but the correction based on relaxation times is introduced in a phenomenological manner that makes it unsuitable for *ab initio* calculations. In this study only the dynamic RA parameterization correctly predicts a finite plasmon lifetime over the entire frequency range. However, outside the electron-hole pair

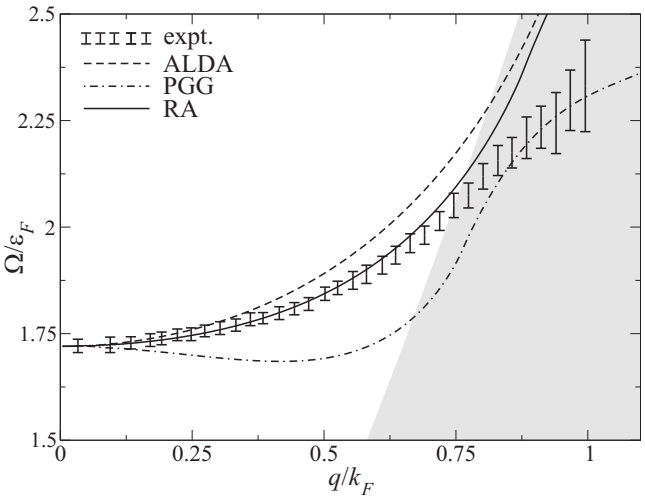

FIG. 5. Calculated plasmon dispersion for $r_s = 4.0$ compared to experimental data for sodium from electron energy-loss spectroscopy (Ref. 32). The theoretical curves have been shifted rigidly to the experimental value at $q = 0$ in order to account for core-polarization effects not included in this electron-gas treatment.

continuum the imaginary part of the plasmon energy is several orders of magnitude smaller than the real part and hence not discernible in the plot.

The good agreement between the static CDOP parameterization on the one hand and the dynamic RA result on the other over a large wavevector and density interval indicates that the frequency dependence of the kernel plays a weak role for the plasmon dispersion. In contrast, the significant discrepancy between static approximations like ALDA that contain the correct long-wavelength limit and others such as PGG, which do not, suggests that a correct parameterization of the wavevector dependence is crucial. Similar conclusions concerning the relative importance of the frequency and wavevector dependence were recently also reported for the correlation energy.[18] This was not entirely surprising, however, because a frequency analysis[18] reveals that the dominant contribution to the energy in any case comes from the low-frequency limit, which is, by design, contained correctly in all static approximations.

To emphasize the error that may arise from an inappropriate kernel, in Fig. 5 we compare theoretical results for $r_s = 4.0$ with experimental data for sodium from electron energy-loss spectroscopy.[32] The theoretical curves have been shifted rigidly to the experimental value at $q = 0$ in order to account for core-polarization effects not included in this electron-gas treatment.[33] At small wavevectors the RA result is in excellent agreement with the experimental dispersion. Although the ALDA correctly reproduces the qualitative features, its growing deviation from the theoretical reference curve soon exceeds the experimental error bars and becomes quite pronounced at intermediate wavevectors. This is even more obvious in the case of PGG. Furthermore, for small wavevectors this parameterization incorrectly predicts a negative dispersion that is not observed in Na, although negative dispersion does occur in heavier alkali metals, such as Cs.[32] The reasons for this anomalous behavior are still controversial.[30,33] Obviously, in such situations a poor parameterization may become a serious obstacle for theoretical interpretations. After the onset of damping due to electron-hole pair excitations, the experimental dispersion flattens slightly. As shown in Fig. 2, the theoretical results exhibit the same effect, but the unshifted RA and ALDA curves only cross the border of the damped regime at larger critical wavevectors. Hence in Fig. 5 quantitative agreement cannot be expected for large wavevectors due to the different physical situations. The PGG curve, on the other hand, lies below the RA result and consequently enters the damped regime at a smaller critical wavevector, but the good agreement with the experimental dispersion for large wavevectors in Fig. 5 is clearly fortutious.

V. SUMMARY

In this paper we have tested several common approximations for the exchange-correlation kernel by examining the plasmon dispersion of the homogeneous electron gas. First of all, we have found that the influence of the kernel is indeed significant, giving rise to large differences between the calculated dispersion curves. The ALDA performs reasonably well, although it underestimates dynamic exchange-correlation effects embodied in the kernel and improves only little upon the RPA. A better quantitative scheme is therefore desirable. In this respect our results, in particular the good agreement between the dynamic RA parameterization and the static CDOP kernel, both of which are presumed to be very accurate, suggest that the neglect of the frequency dependence is of little consequence, giving rise to small deviations only at large wavevectors in the electron-hole pair continuum. The error of the ALDA thus stems largely from its local nature, and extensions should focus on a better description of the wavevector dependence. The challenge of this task is illustrated by the fact that some of the explicitly nonlocal parameterizations we considered, notably PGG, actually lead to worse results although they are known to improve excitation spectra in small atoms. This apparent paradox may be understood by the significance of the long-wavelength limit for the homogeneous electron gas, which determines the leading order of the plasmon dispersion and is contained correctly in the ALDA but not in the PGG kernel. In localized systems such as atoms, on the other hand, the long-wavelength limit is less relevant, whereas dynamic exchange effects contained in the PGG kernel may play an important role. This lack of transferability should encourage specific approximations for solids. The CDOP kernel, which derives from the homogeneous electron gas, seems a step into the right direc-

tion, although its performance for real materials has not been fully explored yet. Finally, we demonstrated that exchange-correlation kernels optimized for small atoms may lead to quantitative, and occasionally qualitative, deviations in the plasmon dispersion for solids that significantly exceed the corresponding experimental error bars and may affect theoretical interpretations.

ACKNOWLEDGMENTS

This work was funded in part by the EU through the NANOPHASE Research Training Network (Contract No. HPRN-CT-2000-00167). We thank M. Fuchs for a careful reading of the manuscript.

---

* Electronic address: tatar@fhi-berlin.mpg.de

[1] P. Hohenberg and W. Kohn, Phys. Rev. **136**, B864 (1964); W. Kohn and L. J. Sham, Phys. Rev. **140**, A1133 (1965).
[2] R. M. Dreizler and E. K. U. Gross, *Density Functional Theory* (Springer, Berlin, Heidelberg, 1990).
[3] E. Runge and E. K. U. Gross, Phys. Rev. Lett. **52**, 997 (1984).
[4] M. Petersilka, U. J. Gossmann, and E. K. U. Gross, Phys. Rev. Lett. **76**, 1212 (1996).
[5] F. Aryasetiawan and O. Gunnarsson, Rep. Prog. Phys. **61**, 237 (1998).
[6] M. E. Casida, K. C. Casida, D. R. Salahub, Int. J. Quantum Chem. **70**, 933 (1998).
[7] S. Hirata and M. Head-Gordon, Chem. Phys. Lett. **302**, 375 (1999).
[8] D. Sundholm, Chem. Phys. Lett. **302**, 480 (1999).
[9] V. Olevano, M. Palummo, G. Onida, and R. Del Sole, Phys. Rev. B **60**, 14 224 (1999).
[10] F. Kootstra, P. L. de Boeij, and J. G. Snijders, J. Chem. Phys. **112**, 6517 (2000).
[11] A. A. Quong and A. G. Eguiluz, Phys. Rev. Lett. **70**, 3955 (1993); A. Fleszar, A. A. Quong, and A. G. Eguiluz, Phys. Rev. Lett. **74**, 590 (1995).
[12] W. Ku and A. G. Eguiluz, Phys. Rev. Lett. **82**, 2350 (1999); A. G. Eguiluz, W. Ku, and J. M. Sullivan, J. Phys. Chem. Solids **61**, 383 (2000).
[13] M. A. Cazalilla, J. S. Dolado, A. Rubio, and P. M. Echenique, Phys. Rev. B **61**, 8033 (2000).
[14] C. J. Umrigar and X. Gonze, Phys. Rev. A **50**, 3827 (1994).
[15] M. E. Casida, C. Jamorski, K. C. Casida, and D. R. Salahub, J. Chem. Phys. **108**, 4439 (1998).
[16] K. Burke, M. Petersilka, and E. K. U. Gross, in *Recent Advances in Density Functional Methods*, edited by P. Fantucci and A. Bencini (World Scientific, Singapore, in press), Vol. III.
[17] M. Corradini, R. Del Sole, G. Onida, and M. Palummo, Phys. Rev. B **57**, 14 569 (1998).
[18] M. Lein, E. K. U. Gross, and J. Perdew, Phys. Rev. B **61**, 13 431 (2000).
[19] T. Klüner, H.-J. Freund, V. Staemmler, and R. Kosloff, Phys. Rev. Lett. **80**, 5208 (1998).
[20] G. D. Mahan, *Many-Particle Physics* (Plenum, New York, 1990).
[21] J. Lindhard, K. Dan. Vidensk. Selsk. Mat. Fys. Medd. **28**, no. 8 (1954).
[22] A. Zangwill and P. Soven, Phys. Rev. Lett. **45**, 204 (1980).
[23] C. A. Ullrich, U. J. Gossmann, and E. K. U. Gross, Phys. Rev. Lett. **74**, 872 (1995).
[24] A. Görling, Phys. Rev. A **57**, 3433 (1998).
[25] S. Moroni, D. M. Ceperley, and G. Senatore, Phys. Rev. Lett. **75**, 689 (1995).
[26] C. F. Richardson and N. W. Ashcroft, Phys. Rev. B **50**, 8170 (1994).
[27] J. P. Perdew and Y. Wang, Phys. Rev. B **45**, 13 244 (1992).
[28] D. M. Ceperley and B. J. Alder, Phys. Rev. Lett. **45**, 566 (1980).
[29] J. P. Perdew and Y. Wang, Phys. Rev. B **46**, 12 947 (1992); **56**, 7018(E) (1997).
[30] E. Lipparini, S. Stringari, and K. Takayanagi, J. Phys.: Condens. Matter **6**, 2025 (1994).
[31] N. D. Mermin, Phys. Rev. B **1**, 2362 (1970).
[32] A. vom Felde, J. Sprösser-Prou, and J. Fink, Phys. Rev. B **40**, 10 181 (1989).
[33] F. Aryasetiawan and K. Karlsson, Phys. Rev. Lett. **73**, 1679 (1994).